

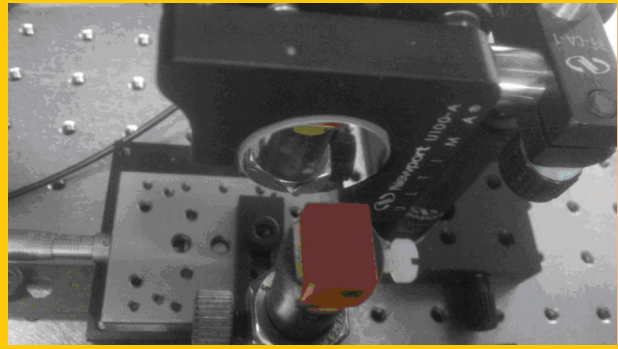
www.lpr-journal.org

LASER & PHOTONICS REVIEWS

WILEY-VCH

REPRINT

Abstract The defect chalcopyrite crystal HgGa_2S_4 has been employed in a 1064-nm pumped optical parametric oscillator to generate <7 ns long idler pulses near 6.3 μm with energies as high as 3 mJ, tunable in a broad spectral range from 4.5 to 9 μm .



High-energy optical parametric oscillator for the 6 μm spectral range based on HgGa_2S_4 pumped at 1064 nm

Adolfo Esteban-Martin^{1,2}, Georgi Marchev¹, Valeriy Badikov³, Vladimir Panyutin¹, Valentin Petrov^{1,*}, Galina Shevyrdyaeva³, Dmitrii Badikov³, Marina Starikova¹, Svetlana Sheina³, Anna Fintisova³, and Aleksey Tyazhev¹

1. Introduction

Notwithstanding the close band-gap values, defect chalcopyrite nonlinear optical crystals with chemical formula $\text{A}^{\text{II}}\text{B}^{\text{III}}_2\text{C}^{\text{VI}}_4$ and point group $\bar{4}$ symmetry exhibit substantially higher second order nonlinear susceptibility compared to their chalcopyrite analogues [1]. However, from this family, only the ternary mercury thiogallate HgGa_2S_4 (HGS) and the quaternary $\text{Cd}_x\text{Hg}_{1-x}\text{Ga}_2\text{S}_4$ (a solid solution of mercury and cadmium thiogallates) have been used so far for phase-matched nonlinear frequency conversion [1]. Comparing HGS to the commercially available chalcopyrite AgGaS_2 (AGS, the standard non-oxide mid-IR material when it comes to pumping down-conversion schemes near 1 μm) its nonlinear coefficient d_{36} is ~ 1.8 times higher and this at slightly increased band-gap value (2.79 eV for HGS against 2.7 eV for AGS), i.e. at somewhat higher damage resistivity [2]. Note that defect chalcopyrites possess a second non-zero tensor component d_{31} but the unknown relative sign in HGS does not allow one to further increase the effective nonlinearity by optimizing the azimuthal angle φ [1].

The wide band-gap of HGS, similar to AGS, means that pumping by short or ultrashort pulse laser sources is possible near 1 μm (e.g. Nd:YAG at 1064 nm) without

two-photon absorption. Most of the other such wide band-gap non-oxide crystals like the biaxial LiGaS_2 , LiInS_2 , LiGaSe_2 , LiInSe_2 , and BaGa_4S_7 exhibit nonlinear susceptibility lower than AGS. Indeed, the relatively new CdSiP_2 (CSP), with chalcopyrite structure, showed exceptionally high nonlinear coefficient and non-critical phase-matching capability but its clear transparency extends only up to ~ 6.5 μm , with an optical damage threshold not superior to that of AGS [2].

Recently, we demonstrated an optical parametric oscillator (OPO) based on HGS which delivered the highest idler output (6.1 mJ at 4.03 μm or 610 mW at a repetition rate of 100 Hz) of any non-oxide nonlinear material pumped at 1064 nm [3], in fact the only millijoule class OPO based on such a wide band-gap non-oxide nonlinear crystal. The main challenge to extend these results to longer wavelengths (where oxide crystals really fail) is the decreasing parametric gain. This makes it difficult to achieve few times above threshold operation before surface damage occurs. Here we demonstrate that HGS presents a perfect combination of properties that enable such operation with type-II phase matching, reaching idler energy of 3 mJ at 6.3 μm which is an improvement of more than 6 times compared to previous best results with CdSiP_2 and BaGa_4S_7 based OPOs [4, 5].

¹ Max-Born-Institute for Nonlinear Optics and Ultrafast Spectroscopy, 2A Max-Born-Str., 12489 Berlin, Germany

² ICFO-Institut de Ciències Fotòniques, Mediterranean Technology Park, 08860 Castelldefels, Barcelona, Spain

³ High Technologies Laboratory, Kuban State University, 149 Stavropolskaya Str., 350040 Krasnodar, Russia

*Corresponding author: e-mail: petrov@mbi-berlin.de

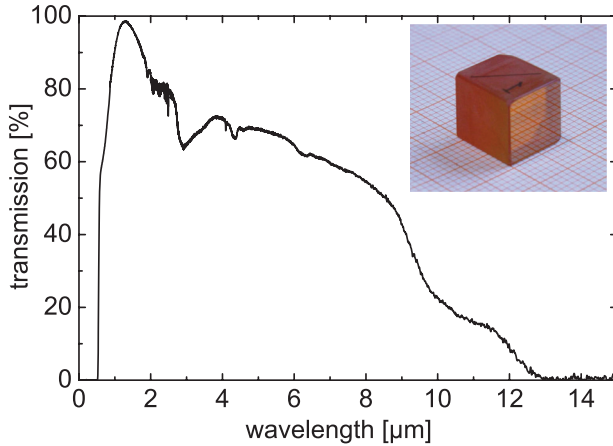


Figure 1 Transmission of the AR-coated HGS crystal. The inset shows a photograph of the OPO element.

2. HGS OPO: experimental results

The HGS element used in the present study was 10.76 mm-long with an aperture of $\sim 9.5 \times 9.5 \text{ mm}^2$, and wedge of $15''$. It was cut at $\theta = 50.2^\circ$ and $\varphi = 0^\circ$ for type-II (eo-e) interaction utilizing only the d_{36} component of the nonlinear tensor. This results in 36% higher effective nonlinearity $d_{\text{eff}} = d_{36} \sin 2\theta$ than type-I. The crystal faces were antireflection-coated (AR) for the signal wavelength range with a single layer of Al_2O_3 (ELAN Ltd.) centered at 1280 nm which reduced substantially the Fresnel losses also at the pump wavelength of 1064 nm, see Fig. 1.

The resulting transmission at 1280 nm was 98% and at 1064 nm it was 94%. This corresponds to absorption losses of $\sim 2\%/cm$ at the signal and pump wavelengths and residual Fresnel reflection of $\sim 2\%$ per surface at 1064 nm. At the idler wavelength of $6.3 \mu\text{m}$ (normal incidence) the AR-coating had no effect on the sample transmission, however, the internal losses were about 10%/cm.

The OPO was pumped by a diode-pumped Q-switched Nd:YAG laser/amplifier system (Innolas GmbH) delivering up to 250 mJ per pulse at 100 Hz, as shown in Fig. 2. The pump pulse duration was typically $\sim 8 \text{ ns}$, the bandwidth 30 GHz (1 cm^{-1}) and the M^2 factor ~ 1.4 . A mechanical shutter (S) with an aperture of 8 mm (nmLaser), was employed to reduce the repetition rate to 10 Hz and thus the average pump power. A half-wave plate (HWP) and a polarizing beam splitter (PBS) were used to attenuate the pump beam and a telescope consisting of two AR-coated lenses with $f_{L1} = -5 \text{ cm}$ and $f_{L2} = 10 \text{ cm}$ was applied to expand it to a diameter of 9.6 and 8.45 mm in the horizontal and vertical directions, respectively. The pump polarization was horizontal and the HGS crystal rotation axis for tuning was vertical.

The pump beam reached the HGS crystal after reflection at the ZnSe bending mirror M2 ($R = 98\%$) and passing through the output coupler (OC) which transmitted 96%. The ZnS OC with radius-of-curvature of -2 m had a transmission of $\sim 30\%$ for the signal wave and 92% for the

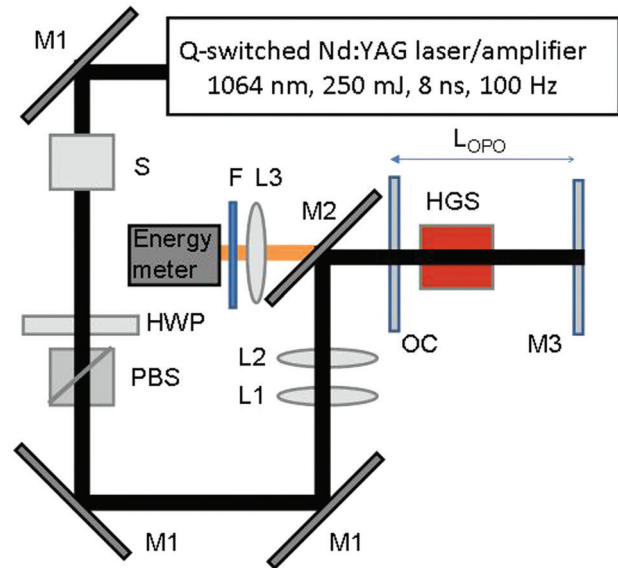


Figure 2 HGS OPO experimental set-up.

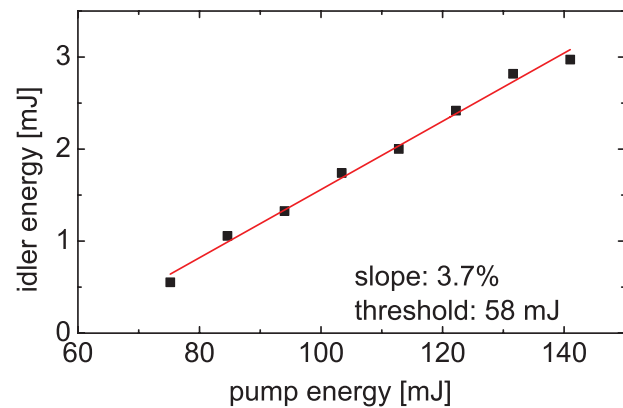


Figure 3 Input-output characteristics of the HGS OPO at normal incidence (idler wavelength of 6300 nm).

idler. A plane Ag-mirror M3 was used as a total reflector for all three waves in a double pump pass singly resonant OPO configuration. The physical cavity length was $L_{\text{OPO}} = 5.2 \text{ cm}$. The $4 \mu\text{m}$ cut-on filter (F) was used to suppress the signal and pump radiation and the $f = 20 \text{ cm}$ BaF_2 lens L3 collected the output idler radiation onto the energy meter. In the following the measured idler energy values were corrected for the transmission of M2 (79%), F, and L3.

Figure 3 shows the input-output characteristics obtained at normal incidence. Only the idler is effectively out-coupled and measured. The threshold of $\sim 58 \text{ mJ}$ corresponds to an axial pump fluence of 0.18 J/cm^2 or a peak intensity of $\sim 23 \text{ MW/cm}^2$. This represents a substantial increase compared to the $4\text{-}\mu\text{m}$ HGS OPO we described in [3] although type-II interaction was employed in the present case to compensate for the reduced parametric gain. The increased threshold is partly due to the longer cavity, however, shorter cavity was not advantageous with respect to achieving higher maximum idler energy because the slope

efficiency was also lower. The maximum idler efficiency with the 5.2 cm long cavity (Fig. 3) reached 2.1% which is equivalent to a quantum conversion efficiency of 12.5%, the slope being equal to 21.9%.

The maximum pump level of ~ 55 MW/cm² axial intensity applied in Fig. 3 was considered to be safe concerning surface damage to the nonlinear crystal because preliminary tests on uncoated and AR-coated plates of HGS revealed a damage threshold of 200–250 MW/cm². However, formation of scattering centers which affect the crystal transmission was detected when the crystal was used in the OPO cavity which was a cumulative irreversible effect depending strongly on the repetition rate and pump level. This was the reason to adopt a repetition rate of 10 Hz in the present study instead of the 100 Hz available from the commercial pump source. Hence, development of such bulk damage (which, when reaching the surface, can lead to fatal surface damage) should be related to the high intracavity signal intensity and could be possibly suppressed in future experiments by further decreasing the OC reflectivity at the signal wavelength. The highest idler energy of 3 mJ obtained with the 5.2 cm long cavity (Fig. 3), corresponds to an improvement of more than 6 times compared to previous best results with CdSiP₂ and BaGa₄S₇ based OPOs [4, 5] and represents the highest idler energy ever demonstrated above 6 μ m with a 1- μ m pumped OPO based on a non-oxide material. It is known that highest conversion efficiencies are achieved at higher ratios of the pump energy to the threshold, however, with the present OPO it was impossible to reach operation 3-times above threshold without bulk damage to the OPO crystal or damage of the Ag total reflector. Higher efficiency and idler energies could be, however, possible using a top-hat shaped pump beam profile which requires a special beam converter. At maximum pump level, the pump depletion measured in the present OPO was about 22.5%, roughly 10% higher than the maximum quantum conversion efficiency. Since no parasitic nonlinear losses were detected for the pump, the difference can be attributed to intracavity losses at the idler wavelength (reflection, absorption, scattering) which are not taken into account when calculating the quantum efficiency from the idler output energy. Although both depletion and conversion efficiency started to saturate from a pump energy of ~ 130 mJ and linear increase of the output energy is expected further, higher conversion efficiency could be achieved with optimized pump, cavity and crystal parameters.

Close to the OPO threshold we measured at normal incidence a signal wavelength of ~ 1280 nm, accordingly the idler wavelength is 6.3 μ m. Figure 4a shows a comparison of the experimental OPO tuning capability with calculations based on the Sellmeier equations for HGS that gave the best agreement [6]. Even not far above threshold the idler tuning range extended from ~ 4.5 to above 9 μ m. The energy dependence in Fig. 4b is in agreement with the parametric gain defined by d_{eff} and the interacting wavelengths. The “anomalous” peak at normal incidence is due to enhanced feedback for the idler wave. In fact this feedback made it possible that the OPO operated without OC: this regime was, however, less efficient and tuning

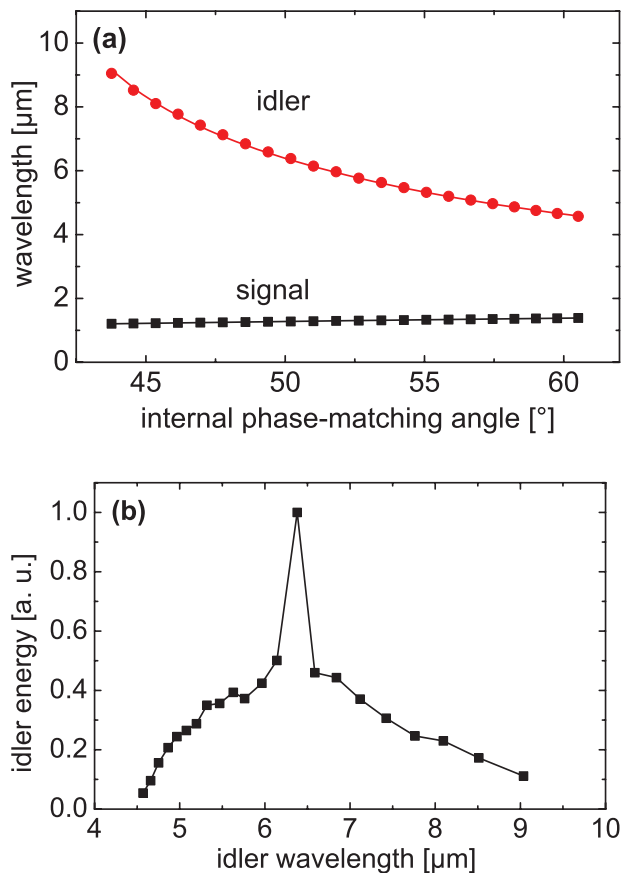


Figure 4 (a) Experimental signal (squares) and idler (circles) OPO wavelengths vs. internal phase-matching angle θ compared with calculations (lines) based on Sellmeier equations [6]. (b) Relative idler energy vs. idler wavelength at pump energy of 80 mJ.

was impossible since the feedback worked only at normal incidence.

We measured the HGS OPO linewidth at the signal wavelength using a 1-mm-thick Ag-coated CaF₂ Fabry-Perot etalon and obtained ~ 2.3 cm⁻¹ or ~ 0.4 nm at 1280 nm. Without OC this linewidth was ~ 5.5 cm⁻¹ or ~ 0.9 nm which is much closer to the calculated spectral acceptance bandwidth of 8.9 cm⁻¹ [6].

The temporal characteristics of the HGS OPO were measured at pump energy of 100 mJ using fast photodiodes and 0.5 GHz oscilloscope. The (HgCdZn)Te detector used for the idler (Vigo systems model PCI-9) had a specified time constant of < 2 ns at 9 μ m but clearly affected the system response at 6.3 μ m. It is obvious that both the signal (~ 6.5 ns) and the idler pulses (< 7 ns) are shorter than the pump pulse duration (Fig. 5).

The M² beam quality factor of the HGS OPO was far above the value corresponding to diffraction limited beams: for the non-resonated idler, two times above threshold, we fitted data measured by the knife-edge method with M² ~ 31.5 in the noncritical and M² ~ 28 in the critical plane. The high M² values can be attributed to a combination of

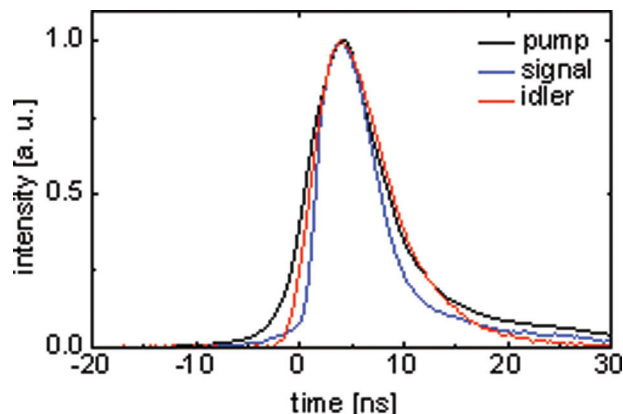


Figure 5 Simultaneously measured temporal pulse profiles of the pump, signal, and idler.

factors including the large pump diameter and the short pump pulse duration [7]. It is, however, ~ 6 times better than in our previous work [3] due to the increased cavity length and it can be expected that this parameter could be substantially improved in the future implementing the RISTRA cavity OPO concept [8].

Finally, we note that although the thermo-optic coefficients of HGS are more than 2 times lower than in AGS, some temperature tuning at normal incidence (see Fig. 4b) is still possible, maintaining the enhanced feedback. Thus, to reach e.g. the idler wavelength of $6.45 \mu\text{m}$ important for surgical applications [8], it is sufficient to heat the crystal to $70^{\circ}\text{--}85^{\circ}\text{C}$. This estimation is based on the dispersion and thermo-optic data from [6, 9] and the interval reflects the deviation between the calculated and the specified cut angle in Fig. 4a for the measured signal wavelength at normal incidence. This deviation is rather small (0.14°) and can be due to the accuracy of the crystal cut which obviously can be easily compensated by slight variation of the crystal temperature.

3. Conclusion

We conclude that HGS has the greatest potential of all known non-oxide nonlinear crystals that can be pumped near $1\text{-}\mu\text{m}$ (powerful Nd- or Yb-based pulsed laser systems) for coverage of the mid-IR wavelength range up to $\sim 12 \mu\text{m}$. The present results indicate that energies $> 5 \text{ mJ}$ at $6.3 \mu\text{m}$ should be possible by better extraction of the idler wave, which includes AR-coatings for the mid-IR and reduction of the residual crystal losses. Reduction of the HGS OPO threshold by using longer crystal samples will dramatically improve the chances to avoid bulk damage formation and

increase the repetition rate to 100 Hz for higher average power. The same can be achieved using flat top pump beam shaping and/or RISTRA cavity design, which has proved to be the best solution for reaching highest idler pulse energies in this mid-IR spectral range from similar OPOs pumped near $2 \mu\text{m}$ [8].

Acknowledgements. The research leading to these results has received funding from the European Community's Seventh Framework Programme FP7/2007-2011 under grant agreement n $^{\circ}$ 224042, from the RFFI (Russia) under grant n $^{\circ}$ 13-02-96500 "Growth and investigations of new nonlinear crystals for the near- and far-IR spectral ranges," and the DLR Project RUS 11/019 (bilateral cooperation with Russia). A. E.-M. acknowledges support from the Catalan Agència de Gestió d'Ajuts Universitaris I de Recerca (AGAUR) through grant (BE-DGR 2011, BE100777) and M. S. acknowledges support from the Federal Target Programme, Russia (contract n $^{\circ}$ 16.522.11.2001) and DAAD Germany (Reg. n $^{\circ}$ 10.72.2012).

Received: 17 July 2013, **Revised:** 18 September 2013,

Accepted: 20 September 2013

Published online: 11 October 2013

Key words: Optical parametric oscillators, mid-infrared, mercury thiogallate.

References

- [1] V. Petrov, V. Badikov, and V. Panyutin, "Quaternary nonlinear optical crystals for the mid-infrared spectral range from 5 to 12 micron," in NATO Science for Peace and Security Series – B: Physics and Biophysics, Mid-Infrared Coherent Sources and Applications, pp. 105–147, Eds: M. Ebrahim-Zadeh and I. Sorokina, (Springer, 2008).
- [2] V. Petrov, *Opt. Mater.* **34**, 536–554 (2012).
- [3] A. Tyazhev, G. Marchev, V. Badikov, D. Badikov, A. Esteban-Martin, G. Shevyrdyaeva, V. Panyutin, and V. Petrov, *Laser Photonics Rev.* **7**, L21–L24 (2013).
- [4] V. Petrov, P. G. Schunemann, K. T. Zawilski, and T. M. Pollak, *Opt. Lett.* **34**, 2399–2401 (2009).
- [5] A. Tyazhev, D. Kolker, G. Marchev, V. Badikov, D. Badikov, G. Shevyrdyaeva, V. Panyutin, and V. Petrov, *Opt. Lett.* **37**, 4146–4148 (2012).
- [6] V. V. Badikov, N. V. Kuzmin, V. B. Laptev, A. L. Malinovsky, K. V. Mitin, G. S. Nazarov, E. A. Ryabov, A. M. Seryogin, and N. I. Schebetova, *Quantum Electron.* **34**, 451–456 (2004).
- [7] G. Anstett, A. Borsutzky, and R. Wallenstein, *Appl. Phys. B* **76**, 541–545 (2003).
- [8] G. Stoeppler, M. Schellhorn, and M. Eichhorn, *Laser Phys.* **22**, 1095–1098 (2012).
- [9] N. Umemura, T. Mikami, and K. Kato, *Opt. Commun.* **285**, 1394–1396 (2012).